THE JOURNAL OF PHYSICAL CHEMISTRY B

ARTICLE

pubs.acs.org/JPCB

Experimental and Theoretical Study on the Intermolecular Complex Formation Between Trehalose and Benzene Compounds in Aqueous Solution

Kota Sakakura,[†] Atsutoshi Okabe,[†] Kazuyuki Oku,[‡,§] and Minoru Sakurai*[,†]

[†]Center for Biological Resources and Informatics, Tokyo Institute of Technology, B-62 4259 Nagatsuta-cho, Midori-ku, Yokohama 226-8501, Japan

[‡]Glycosciene Institute, Research Center, Hayashibara Biochemical Laboratories, Inc., 675-1 Fujisaki, Okayama 702-8006, Japan

Supporting Information

ABSTRACT: The uniqueness of trehalose as a stress protectant may exist in its potential amphiphilic character capable of interacting with both hydrophilic and hydrophobic partners in aqueous solution. To address this issue, we here investigated the interaction between trehalose and aromatic compounds. NMR measurements, including $^{1}H-^{1}H$ NOESY spectra, provide direct evidence for the formation of stable intermolecular complexes of trehalose with benzene (or *p*-cresol) in aqueous solution. In addition, corresponding theoretical evidence is provided by calculating the potential mean force as a function of the distance between trehalose and benzene. In the energy minimum structure, the benzene molecule is located only around the hydrophobic side of trehalose where the first hydration shell is not formed. Therefore, it can be concluded that benzene binds to trehalose in a fashion in which dehydration penalty is minimized. Finally, we discuss the possible biological roles of the trehalose−benzene interaction discovered here.

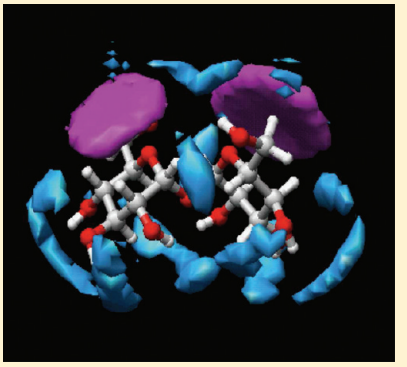

INTRODUCTION

Trehalose, a nonreducing disaccharide consisting of two D-glucose units linked by an α,α-(1→1)-linkage, occurs widely in nature, microorganisms, plants, and invertebrates.[1] Trehalose is well-known to act as a protectant against various environmental stresses, such as desiccation, heat, freezing, or osmotic shock.[2−4] Among them, the mechanism of desiccation tolerance has been extensively studied from both in vivo and in vitro experiments. For example, a large amount of trehalose accumulated in dehydrated larvae of the African sleeping chironomid, *Polypedilum vanderplanki*, is vitrified to stabilize cellular components such as proteins and membranes and simultaneously binds to the membrane surface in place of bound water.[5] Vitrification and water displacement are widely accepted mechanisms in which trehalose protects dried biological molecules/materials.[6,7] In addition to water stress, there is growing evidence that trehalose acts as a protectant against chemical stress like oxidation:[8−13] for example, this sugar effectively depresses the heat- or radical-induced peroxidation of unsaturated fatty acids (UFAs).[8,9,11,12]

The multifunctional properties of trehalose may be ascribed to the presence of the α,α-(1→1)-linkage. Theoretical studies based on molecular mechanics[14−24] or quantum mechanics[25] indicated that there is only one energy minimum for rotation about the ϕ,ψ dihedral angles of the α,α-(1→1)-linkage. In other words, trehalose is restricted to a single stable conformation, whose shape is similar to a clam shell (Figure 1). This has also been confirmed by many experimental studies, including X-ray analysis,[26,27] optical rotation,[28,29] and NMR[30] experiments. Recently, Albertorio et al. indicated that disaccharide molecules containing an α, α-(1→1)-linkage, compared with other disaccharides, are effective at retaining the bilayer structure in the absence of water. They inferred that the specific arrangement of the hydroxyl groups in trehalose may optimize the hydrogen-bonding arrangement for water replacement. The lack of flexibility of the α,α-(1→1)-linkage results in higher glass transition temperature and kinetically stable glassy matrix, leading to marked antidesiccant properties of trehalose. The antioxidant function against UFAs as mentioned above was observed uniquely for trehalose: other disaccharides with other types of glycosidic bonds, such as maltose (α,β-(1→4)) and neotrehalose (α,β-(1→1)), do not have such a function.[9]

For a glucose residue, with all of its hydroxyl groups in the equatorial position in the $^{4}C_{1}$ conformation, the "top" and "bottom" of the molecule are hydrophobic, made up of aliphatic C−H surfaces, while the equatorial periphery is quite hydrophilic. By combining such an amphiphilic property of the glucose unit with the conformational rigidity of the glycosidic bond, trehalose has a unique hydration structure. Choi et al. demonstrated that water molecules are distributed in a highly anisotropic fashion around trehalose: the open side of a clam shell

Received: April 21, 2011
Revised: June 30, 2011
Published: July 09, 2011

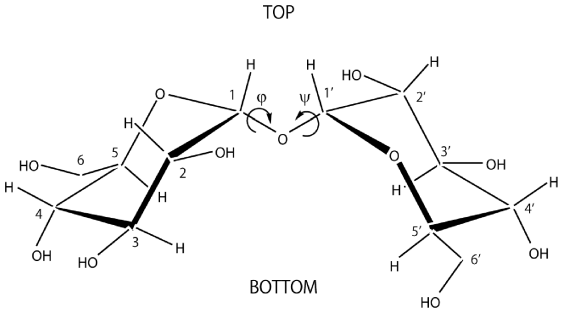

Figure 1. Structure and atom numbering of trehalose.

(hereafter abbreviated as "bottom" side, Figure 1) is hydrated, but the hinge portion of the clam shell ("top" side) is less hydrated.[24] More than 20 years ago, Rudolph et al. pointed out that trehalose can form energetically stable comformations with phospholipids through hydrophobic interactions.[31] These facts suggest that trehalose has an amphiphilic character in itself and would be able to interact with both hydrophilic and hydrophobic partners, probably contributing to the multifunctional character of trehalose.

About one decade ago, Brady's group investigated the interaction between glucose and benzene in aqueous solution using molecular dynamics simulation.[32] Their potential of mean force (PMF) data clearly indicated that the two molecules form a stacked type of intermolecular complex. By reference to X-ray structures of various sugar-binding proteins,[33−35] they discussed that these proteins may recognize sugar molecules through interactions of hydrophobic residues, for example, Phe and Trp, with the hydrophobic surface of the sugars. These findings suggest that trehalose could form a stable intermolecular complex with benzene as if it were a hydrophobic molecule. According to studies on the antioxidant function mentioned above,[8,10−12] trehalose can form intermolecular complexes with UFAs possessing *cis*-olefin double bonds such as linoleic acid and α-linolenic acid, but no apparent interaction was observed for UFAs with a *trans* double bond. Considering that the *cis* type of double bond is similar to a part of the benzene molecule in shape, it is also expected that a trehalose−benzene complex is formed in aqueous solution.

In this study, we provide experimental and theoretical evidence that trehalose can form stable intermolecular complexes with benzene compounds in aqueous solution. First, experimental evidence is provided from NMR measurements, including ^{1}H-T_1 and ^{1}H−^{1}H NOESY, for a mixture of trehalose and benzene (or *p*-cresol). On the other hand, to obtain theoretical evidence, we calculated the PMF as a function of the distance (R) between the center of mass of trehalose and that of benzene (or *p*-cresol). PMF will exhibit a single minimum at a value of $R \approx 5$ Å, indicating the formation of a stable intermolecular complex. Interestingly, our simulation data indicate that in such a minimum energy structure the benzene molecule is located only around the "top" side of trehalose (Figure 1). To elucidate the driving force for the formation of such an intriguing intermolecular complex, we compare the spatial distribution of benzene around trehalose with the hydration structure of the sugar. Dehydration pockets were shown to be present around the top side of trehalose and the positions of such pockets coincide with the regions where the above benzene molecule is located with a high probability. Similar results are obtained for the trehalose−*p*-cresol mixture in aqueous solution, although the *p*-cresol molecule is slightly distributed also on the bottom side of trehalose. In conclusion, benzene and *p*-cresol, models of the side chains of Phe and Tyr, respectively, are able to bind to trehalose in a manner such that dehydration penalty, accompanied by intermolecular complex formation, is minimized. Finally, we discuss possible biological roles of such intermolecular complex formation between trehalose and aromatic compounds.

MATERIALS AND METHODS

Chemicals. Trehalose (>99.9% purity), neotrehalose (α-D-glucopyranosyl β-D-glucopyranoside, 99.8%), nigerose (2-O-α-D-glucopyranosyl-D-glucose, 97.0%), kojibiose (3-O-α-D-glucopyranosyl-D-glucose, 98.0%), maltose (4-O-α-D-glucopyranosyl-D-glucose, 99.9%), and isomaltose (6-O-α-D-glucopyranosyl-D-glucose, 99.9%) were produced by Hayashibara Biochemical Laboratories, Inc., Okayama, Japan. Benzene was purchased from Wako Pure Chemical Industries, Osaka, Japan. These chemicals were used without further purification.

NMR Experiments. For NMR experiments, we prepared the D_2O (D, 99.9%, Cambridge Isotope Laboratories, MA) solutions of trehalose/benzene mixtures with their molar ratio ranging from 0 to 18, where the absolute concentration of benzene was kept constant at 8.31 mM. The NMR measurements were done at 25 °C by using an FT-NMR spectrometer (model JMN-AL300, Nihon Denshi Co. Tokyo, Japan), operating at 300.4 MHz (^{1}H frequency). The ^{1}H (δ) were measured with respect to the ^{1}H signals of tetramethylsilane (Wako Pure Chemical Industries) dissolved in the samples, respectively. The spin−lattice relaxation time of ^{1}H (hereafter abbreviated as ^{1}H-T_1) was measured using a conventional inversion−recovery pulse sequence, that is, a repeated 90°−τ−90° pulse. The repetition time was taken to be always 5 times greater than T_1. For both ^{1}H-T_1, the signal recovery was a single-exponential decay. The ^{1}H-T_1 measurements were performed for major ^{1}H peaks assigned to benzene. ^{1}H−^{1}H NOESY spectra were obtained for the mixture of trehalose and benzene (molar ratio of 2:1). NOE measurements were performed using the pulse sequence depicted below

$$^1\mathrm{H}: 90°\text{-}t_1\text{-}90°\text{-}\tau_m\text{-}90°\text{-}ACQTM\text{-}$$

where the mixing time τ_m was 5 s and the acquisition time ACQTM was 2.7 s. The NMR data were processed by using a software package, Alice WINNMR 2.1, attached to the NMR apparatus.

Calculations. The glycosidic dihedral angles of the initial structure of trehalose were set to be equal to those obtained from NMR analysis,[30] that is, ($\phi_{H(1)-C(1)-O(1)-C(1')}$, $\psi_{H(1')-C(1)-O(1)-C(1)}$ = (−41°, −41°)). Subsequently, this structure was optimized by the HF/6-31G** level of calculation, and then we obtained a more stable structure with the glycosidic dihedral angles of ($\phi_{H(1)-C(1)-O(1)-C(1')}$, $\psi_{H(1')-C(1)-O(1)-C(1)}$ = (−65°, −65°)), which was used as an initial structure for the MD simulation. The atomic charges of trehalose were evaluated by the MP2/6-31G** level of calculation for this stable structure. The initial structure and atomic charges of benzene were also obtained according to the same computational protocol as for trehalose. All quantum chemical calculations were carried out using the Gaussian03 program.[36] For both trehalose and benzene, force field parameters other than the atomic charges were taken from the general Amber force fields (GAFF)[37] and the water molecule was approximated by the TIP3P model.[38]

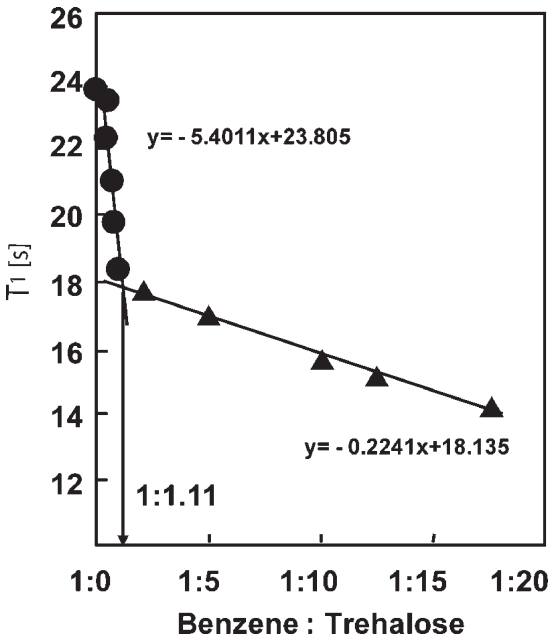

Figure 2. ^{1}H-T_1 values of benzene plotted against the molar ratio of trehalose to benzene.

The free energy profile for the trehalose/benzene complexation process was obtained from the PMF curve as a function of the distance (R) between the centers of mass of the two solute molecules. Before performing umbrella sampling simulations to obtain such a PMF curve, we first prepared the initial system as follows: (1) one molecule of trehalose and that of benzene, with their geometries as determined above, were arranged so that the distance R was 3.6 Å, (2) this 1:1 complex was placed in a rectangular box with a size of 37 × 36 × 35 Å, (3) a total of 997 water molecules were placed into the box, and (4) the resultant system was subjected to energy minimization with the steepest decent method, and a subsequent 100 ps MD run for equilibration of the system at 298 K by constraining the atomic positions of trehalose and benzene with a large spring constant of 100 kcal/mol Å^{-2}. Next, PMF was obtained using the umbrella sampling MD simulation, where the distance R was changed in a 0.2 Å interval from 3.6 to 13.0 Å, and at each step, the distance was fixed with an umbrella potential of 5.0 kcal/mol Å^{-2}. In other words, we performed MD simulations with 48 windows, each of which was run for 500 ps. It was confirmed that adjacent windows overlapped well (see Figure S1 of Supporting Information). By reference to the autocorrelation function for the overall tumbling motion of trehalose (Figure 5 of ref 24), a 500 ps umbrella simulation for each window may not be enough for the reorientational relaxation of this sugar. So, for the trehalose-benzene system, we also performed another series of umbrella sampling simulation with a 2 ns run for each window. The free energy curve along the reaction coordinate R was obtained by performing the weighted histogram analysis method (WHAM)[39] for the results of all the umbrella sampling MD simulations.

To investigate the hydration property of pure trehalose, we performed another MD simulation for an aqueous solution of pure trehalose. Then, one molecule of trehalose and 807 water molecules were placed into a unit cell box with a size of 36 × 32 × 33 Å. The resultant system was subjected to energy minimization with the steepest decent method, and a subsequent 100 ps MD run for equilibration of the system at 298 K. After this, the production run was performed for 40 ns.

All MD simulations were carried out using the Amber8 program package[40] under the following conditions: (1) NPT ensemble (1 atm, 298 K), (2) Berendsen's methods[41] for controlling temperature and pressure, (3) particle mesh Ewald method[42] for calculating long-range interactions, and (4) SHAKE methods[43] for constraining the hydrogen atoms bound to heavy atoms.

Table 1. Effect of Disaccharides on the Spin-Lattice Relaxation Time (T_1) of Benzene and *p*-Cresol

	T_1 /s					
		p-cresol				
disaccharide	benzene	H-3,5		H-2,6		CH_3
trehalose	14.0	4.41	4.26	5.28	5.54	2.40
neotrehalose	22.5	5.41	5.65	7.18	8.00	2.44
kojibiose	21.1	5.38	5.41	7.15	7.58	2.44
nigerose	23.2	5.39	5.58	7.19	7.75	2.43
maltose	20.8	5.34	5.78	7.15	7.68	2.43
isomaltose	19.8	5.41	5.54	7.14	7.98	2.47
no addition	23.6	5.38	5.75	7.18	7.99	2.49

RESULTS

NMR Analysis. First, to examine whether or not the interaction between trehalose and benzene occurs in aqueous solution, we carried out NMR experiments. In Figure 2, the ^{1}H-T_1 of benzene is plotted against the molar ratio of trehalose to benzene. Interestingly, the ^{1}H-T_1 value increased steeply to a molar ratio of about 1 with a slope of −5.4, while it changed more slowly in the higher molar ratio region (slope was −0.22). The present NMR measurements were carried out under the so-called extremely narrowing conditions; a decrease in the T_1 value signifies a decrease in the mobility of a molecule and molecular fragment. Thus, the result of Figure 2 indicates the lowering of molecular motion of benzene with an increasing concentration of trehalose, which implies the occurrence of some intermolecular interactions between them. The presence of an inflection point at a 1:1 molar ratio suggests that complexation may occur with a 1:1 stoichiometry. This is very similar to our previous result in which a stable 1:1 intermolecular complex was formed between trehalose and a *cis* double bond in unsaturated fatty acid or diene in aqueous solution.[11,12] From Figure 2, the binding constant was estimated to be 1.07 × 10^3 M^{-1} at 298 K, corresponding to a binding free energy of −4.16 kcal/mol.

Similar ^{1}H-T_1 measurements were performed for mixtures of benzene and other disaccharides such as maltose, neotrehalose, kojibiose, nigerose, or isomaltose, in which the sugar/benzene molar ratio was set at 18 in all cases. As shown in Table 1, dissacharides other than trehalose exhibited no significant effect on the ^{1}H-T_1 of benzene. It is therefore inferred that only trehalose could form an intermolecular complex with benzene among the disaccharides studied. ^{1}H-T_1 measurements were also carried out for *p*-cresol−disaccharide mixtures. In this case, the T_1 values of H-2,6 and H-3,5 protons of *p*-cresol were drastically decreased by the addition of trehalose, although they underwent no significant changes when other disaccharides were added

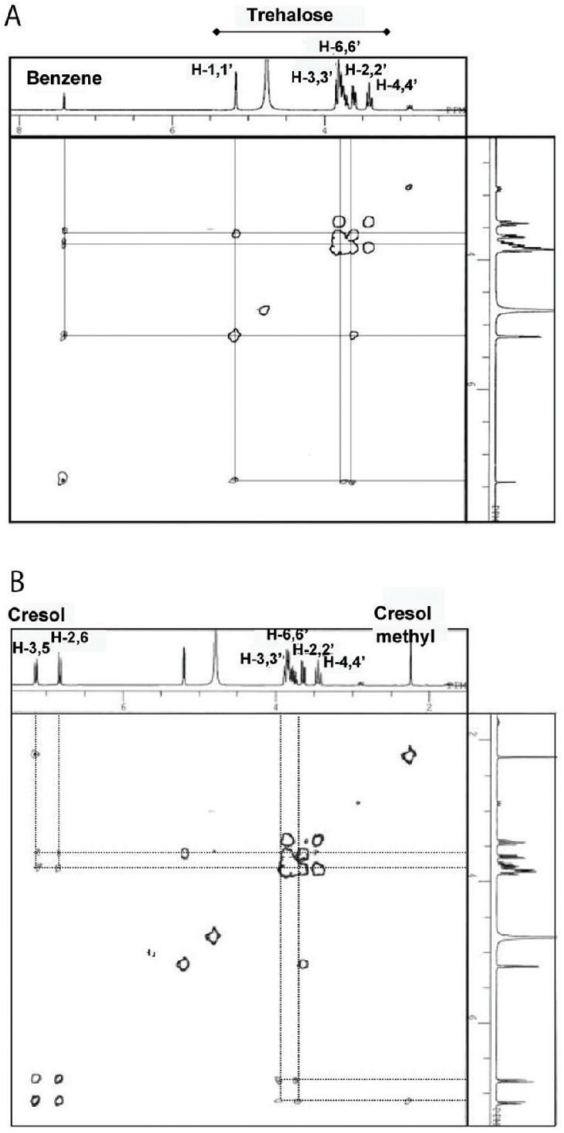

Figure 3. $^{1}H-^{1}H$ NOESY spectra of a mixture of trehalose and benzene (A) and of a mixture of trehalose and *p*-cresol (B). In both cases, trehalose was added in excess with a molar ratio of 18.

(Table 1). Thus, the uniqueness of trehalose was also confirmed for the interaction with *p*-cresol.

To obtain more detailed information about the trehalose/benzene (or *p*-cresol) complex, we measured the $^{1}H-^{1}H$ NOESY spectrum of a mixture of trehalose and benzene with a trehalose/benzene molar ratio of 18. As shown in Figure 3A, clear cross-peaks were observed between the benzene proton signal (7.43 ppm) and the 1(1′)-, 2(2′)-methine or 6(6′)-methylene proton signals of trehalose. The CH protons at the 1, 2, and 6 positions are all located on the top side of trehalose (Figure 1). Therefore, the results of Figure 3A suggest that a benzene molecule is distributed around a trehalose molecule in a highly anisotropic fashion with a high probability on the top side. For the trehalose−*p*-cresol system, a clear cross peak was observed between the aromatic proton signals (H-3,5 and H-2,6) of *p*-cresol and the 2(2′)-proton of trehalose (Figure 3B). In addition, cross peaks were also observed between these *p*-cresol proton signals and the band involving the 3(3′)- and 6(6′)-proton

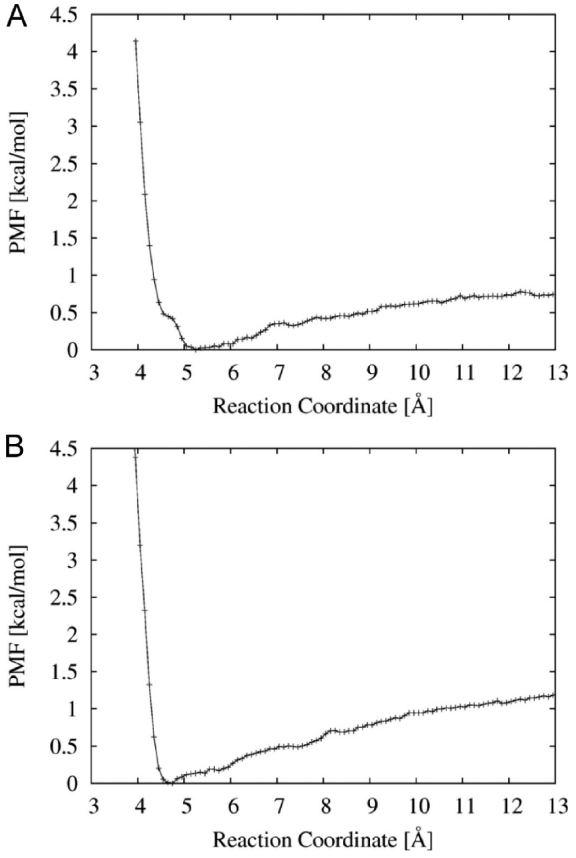

Figure 4. PMF curves for the trehalose−benzene system (A) and for the trehalose−*p*-cresol system (B).

signals of trehalose: the latter two signals are partially overlapping with each other. The H-3 proton of trehalose is located on the bottom side (Figure 1). Thus, in contrast to benzene, a *p*-cresol molecule is thought to be distributed partially on the bottom side. From the experimental results alone, it is difficult to obtain more detailed structural information about the complex, and thus we performed molecular dynamics simulations as described next.

Computational Analysis. Figure 4A and B depict the PMF curves for the trehalose−benzene and trehalose−*p*-cresol systems, respectively. The PMF of the trehalose−benzene system has the single minimum located at R = 5.2 Å, with a stabilization energy of about 0.8 kcal/mol. Figure S2 of Supporting Information shows the PMF curve obtained with a 2 ns umbrella simulation for each window, where the minimum again appears at R = 5.2 Å with a depth of 0.75 kcal/mol. This implies that the actual parameter values characterizing the PMF curve rapidly converges with respect to the simulation time for each window. In the trehalose−*p*-cresol system, the minimum appears at R = 4.6 Å with a stabilization energy of 1.1 kcal/mol. These results are the direct theoretical evidence that trehalose can form a stable intermolecular complex with benzene and *p*-cresol in aqueous solution, consistent with the above NMR results. The position of the PMF minimum for the trehalose−*p*-cresol system is shifted to the left by about 0.6 Å compared with that for the trehalose-benzene system, accompanied by an increase in the depth. This observation suggests that the former complex is more stable than the latter, although the difference is not so large.

At this stage, it was of interest to examine the structures of these intermolecular complexes at the atomic level. For this

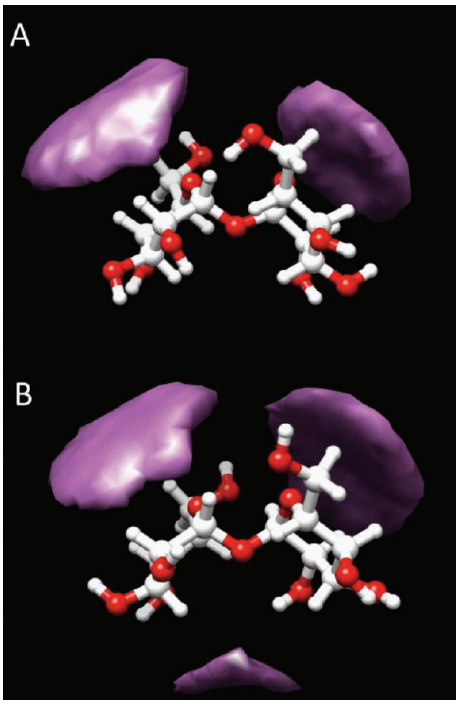

Figure 5. Iso-probability surface of the center of mass of benzene around trehalose (A) and that of the center of mass of *p*-cresol around trehalose (B).

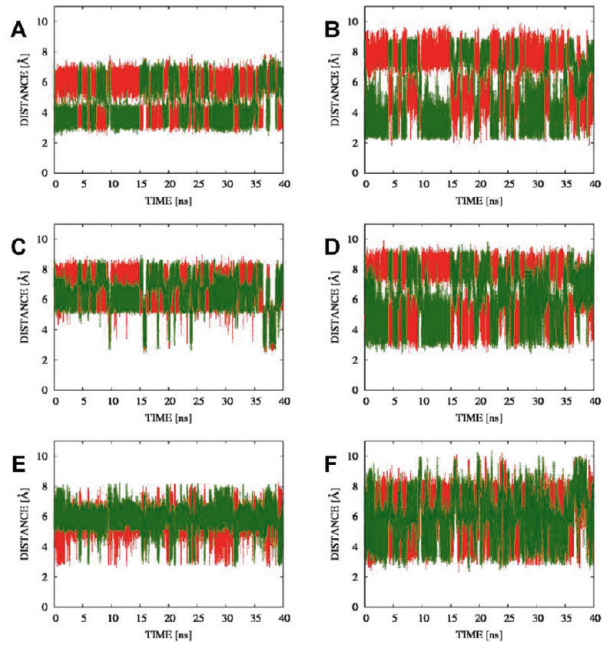

Figure 6. Time evolution of the distance between the center of mass of benzene and the methyne and methylene hydrogen atoms of trehalose: (A) H-1(1′), (B) H-2(2′), (C) H-3(3′), (D) H-4(4′), (E) H-5(5′), (F) H-6(6′).

purpose, we performed a 40 ns MD simulation for the aqueous solution of a 1:1 trehalose−benzene complex, where the distance *R* was constrained to 5.2 Å and the other geometrical parameters were unconstrained except for the motions of hydrogen atoms

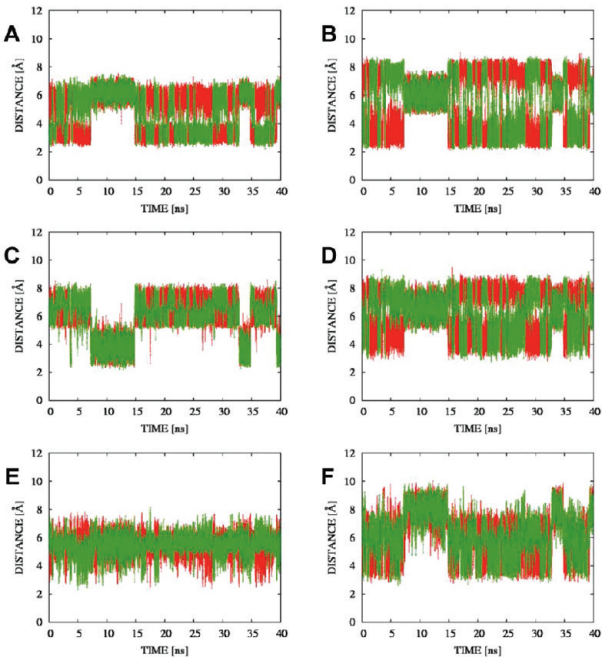

Figure 7. Time evolution of the distance between the center of mass of *p*-cresol and the methyne and methylene hydrogen atoms of trehalose: (A) H-1(1′), (B) H-2(2′), (C) H-3(3′), (D) H-4(4′), (E) H-5(5′), (F) H-6(6′).

bound to heavy atoms. Using the trajectory data obtained, we analyzed the spatial distribution of the benzene molecule around trehalose. Figure 5A shows the iso-probability surface of the center of mass of benzene around trehalose. Interestingly, the benzene molecule was most frequently located on the top side of trehalose throughout the MD run but was rarely found on the bottom side. Similarly, we performed a 40 ns MD simulation for the trehalose−*p*-cresol complex, where the distance *R* was constrained to 4.6 Å. As shown in Figure 5B, the *p*-cresol molecule is located mostly on the top side, although sparsely distributed on the bottom side.

Next, to compare these simulation results with the ^{1}H−^{1}H NOESY results mentioned above, we measured the distance between the CH or CH_2 hydrogen atoms of trehalose and the center of mass of benzene or *p*-cresol. Figure 6 shows the time evolution of the distance between benzene and the 1(1′)-H, 2(2′)-H, 3(3′)-H, 4(4′)-H, 5(5′)-H, or 6(6′)-H of trehalose in the trehalose−benzene system, where 6(6′)-H are the hydrogen atoms of the exocyclic methylene group and the results for the two equivalent glucose units of trehalose are discriminated by color (red or green). As can be seen, the benzene molecule is always located near either 1-H or 1′-H with a minimum distance of about 3 Å throughout the simulation. Similarly, benzene is located near either 2-H or 2′-H, either 4-H or 4′-H, and either 6-H or 6′-H. However, benzene rarely approaches the 3(3′)H site: the corresponding distance is maintained longer than 5 Å during most of the simulation time. At the 5(5′)H site, benzene approaches trehalose more frequently than it does at the 3(3′)H site, but the frequency is much less than that observed for the 1(1′)-H, 2(2′)-H, 4(4′)-H, and 6(6′)-H sites. It should be noted that these four kinds of hydrogen atoms are located on the outside surface of the clam shell-like structure of trehalose (Figure 1). Combining these results, it can be said that the

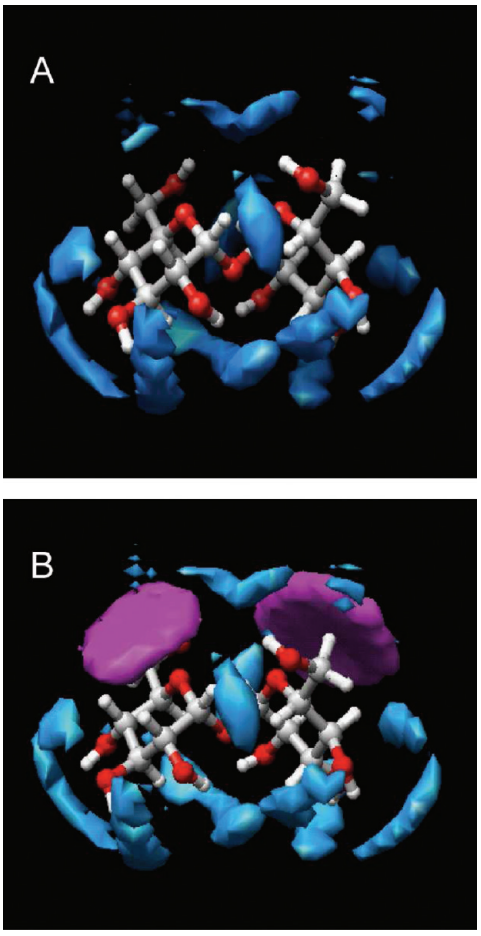

Figure 8. (A) Distribution of water molecules around trehalose. Cloud-like regions represent iso-probability surface of water oxygen atoms. (B) Superimposition of Figure 5A on (A).

benzene moves between the top sides of the two glucose units in a shuttle-like fashion, leading to the distribution shown in Figure 5A. Generally, in $^{1}H-^{1}H$ NOESY measurements, the proton−proton pair can be detected as a cross peak if its distance is less than 5 Å. Thus, according to our simulation results, cross peaks were expected to be observed between the benzene signal and the 1(1′)-H, 2(2′)-H, 4(4′)-H, and 6(6′)-H signals of trehalose, but not the 3(3′)-H signal. This is in fairly good agreement with the experimental results shown in Figure 3A.

Distance data for the trehalose−*p*-cresol system is shown in Figure 7. In this case, the *p*-cresol molecule can visit the 3(3′)-H site frequently; for example, the minimal distance is about 3 Å in the time regions of 7−15 and 33−35 ns. Whenever *p*-cresol approaches 3(3′)-H, it is away from the 1(1′)-H, 2(2′)-H, 4(4′)-H, and 6(6′)-H sites. Taken together, it has a shuttle-like motion between the top and bottom sides of trehalose, leading to the distribution shown in Figure 5B. Therefore, in the trehalose−*p*-cresol system, an NMR cross peak should be observed for 3(3′)-H in addition to 1(1′)-H, 2(2′)-H, 4(4′)-H, and 6(6′)-H, consistent with the experimental data shown in Figure 3B.

Our next interest was the reason why benzene binds to trehalose in a fashion shown in Figure 5A. To address this, we performed a MD simulation for an aqueous solution of pure trehalose and examined the distribution of water molecules surrounding it. As shown in Figure 8A, water molecules are distributed on the bottom side with a high density, while on the top side there are regions in which hydration shells are not formed regularly. In other words, dehydrated pockets are present. Roughly speaking, there is one dehydration pocket for each glucose unit. Such a highly anisotropic water distribution around trehalose has been already reported in previous studies.[17,24] By superimposing Figure 5A upon Figure 8A, we obtained Figure 8B. As can be seen, the dehydration pockets coincide with the regions where benzene is located with a high probability. Taken together, it can be interpreted that the benzene molecule binds to trehalose in a unique fashion such that dehydration penalty, accompanied by intermolecular complex formation, is minimized. The OH group of *p*-cresol would form hydrogen bonds with the OH group of trehalose in place of water molecules. Thus, *p*-cresol can visit the hydrophilic side (bottom side) of trehalose, including the 3(3′)-H sites, consistent with the above NMR data.

DISCUSSION

In previous studies,[11,12] we found that trehalose can form a stable intermolecular complex with unsaturated compounds possessing the *cis*-type olefinic double bond. This fact motivated us to investigate whether or not benzene and its related compounds also bind to trehalose in aqueous solution, because their unsaturated bonds are similar in shape to the *cis*-type double bond. As expected, the present NMR and MD simulation results provided clear evidence on the complex formation of trehalose with benzene and *p*-cresol. It should be stressed that such complex formation was not observed for any disaccharide other than trehalose. Thus, it is important to discuss the origin of such a unique nature of trehalose.

As shown in Figure 8B, the aromatic ring approaches the dehydrated (hydrophobic) pocket located on the top side of trehalose. In general, a glucose residue, with all of its hydroxyl groups in the equatorial position in the $^{4}C_{1}$ conformation, is hydrophobic on its top and bottom sides because these sides are made up of aliphatic C−H surfaces. Thus, all disaccharides composed of glucose residues should have hydrophobic pockets similar to trehalose. However, in the disaccharides other than trehalose, rotational motions (conformation changes) would occur around the glycosidic bonds because there are more than two energy minima about the dihedral angles (ϕ, ψ) of the glycosidic linkage.[15] As a result, the orientations of the hydrophobic pockets should fluctuate violently, a situation of which does not favor the formation of intermolecular complexes with other molecules such as benzene. In contrast, the α,α-(1→1)-linkage of trehalose has a single energy minimum around the rotation of the glycosidic bond,[14−25] and this sugar has only one conformation in solution,[28−30] leading to a favorable and stable interaction with benzene. Comparison of the molecular motions about the dihedral angles (ϕ, ψ) between trehalose and neotrehalose is given in Figure S3 of Supporting Information. Taken together, the structural rigidity arising from the presence of the α,α-(1→1)-linkage is thought to be the main origin generating the above uniqueness of trehalose.

In aqueous solution, a benzene molecule would first approach the top side region of a trehalose molecule without apparent dehydration penalty and subsequently make contact with it probably through van der Waals interactions. To examine to what extent such an intermolecular complex is stable, we evaluated the interaction energies for several structures sampled

Table 2. Trehalose−Benzene Interaction Energies (ΔE) Calculated for Four Structures Randomly Picked up from the Trajectory of the MD Simulation for Their Complex State

	Energy of Quantum Chemical Calculation[a]			
	structure A[b]	structure B[b]	structure C[b]	structure D[b]
trehalose (a.u.)	−1294.2870	−1294.2481	−1294.2722	−1294.2784
benzene (a.u.)	−231.4922	−231.4929	−231.4981	−231.4995
complex (a.u.)	−1525.7877	−1525.7510	−1525.7808	−1525.7874
ΔE (kcal/mol)	−5.39	−6.24	−6.59	−5.96
	Energy of Molecular Mechanics Calculation[c]			
E_{el} (kcal/mol)[d]	−0.30	−0.91	−0.96	−0.57
E_{vdW} (kcal/mol)[e]	−4.57	−4.58	−4.45	−4.72
ΔE (kcal/mol)	−4.86	−5.49	−5.42	−5.3

[a] Obtained from the MP2/6-31G** level of calculation. [b] Figures of these structures are given in Figure S4 in the Supporting Information. [c] Obtained using the Amber force field. [d] Electrostatic energy between trehalose and benzene. [e] van der Waals energy between trehalose and benzene.

from the trajectory of the 40 ns MD simulation for the trehalose−benzene 1:1 complex with a constraint of R = 5.2 Å. The trehalose−benzene interaction energy was obtained from two types of calculations: one is the MP2/6-31G** level of quantum chemical calculation and the other is the molecular mechanics calculation with the Amber force field. As shown in Table 2, the calculations exhibited a stabilization energy of about 4.9−6.5 kcal/mol with a dominant contribution of the van der Waals energy, a value which is close to a stabilization energy of 4.16 kcal/mol calculated from the experimental binding constant.

In a previous study by Brady's group,[32] a PMF curve was obtained for a glucose−benzene system by keeping the two molecules in the parallel stacked arrangement thus exhibiting a primary minimum at 4.2 Å. In the present study, PMF calculations were carried out without imposing any restraint on the relative orientation between the glucose residue of trehalose and benzene (or *p*-cresol). As a result, it was shown that a *p*-cresol molecule can also be located near the open side of the clam shell structure of trehalose in addition to the top side. According to Figure 8A, water molecules form regular hydrogen bond networks with the OH groups of trehalose in this region. Unlike benzene, *p*-cresol seems to approach this region by forming hydrogen bonds with the trehalose OH groups, especially 3(3′)-OH groups, in place of bound water molecules.

Brady's group pointed out that the parallel stacked-type interaction, as observed for the glucose−benzene system, would play an important role when proteins that bind carbohydrates recognize substrates and increase their affinity for these substrates.[32] In fact, the binding sites of proteins that recognize glucose residues contain hydrophobic residues such as phenylalanine or tryptophan, probably to provide an extended hydrophobic surface for the nonpolar faces of the sugars to dock against.[33−35] Recently, it has been reported that mono- and disaccharides are capable of CH/π stacking onto the DNA base pair of a duplex, which may be a fundamental part of some drug−DNA recognition process.[44] As described in the Introduction, nowadays trehalose is utilized in various scientific and industrial fields, including medicinal, pharmaceutical, food, and cosmetics, among others. The trehalose−aromatic residue interaction studied here is expected to play an important role in some of these applications. An example is the inhibition effect of trehalose on protein aggregation.[45−49] An in vitro study by Liu et al. clearly indicated that trehalose effectively inhibits the aggregation of β-amyloid (Aβ) 40 and 42.[47] Although the underlying mechanism for such phenomena is far from being fully understood at present, a key to solving this issue may exist in a specific interaction with aromatic compounds, as studied here. Biochemical mutational studies indicated that the Aβ_{16-22} fragment (Ace-Lys-Leu-Val-Phe-Phe-Ala-Glu-NH_2) is critical for the assembly of full-length Aβ, that is, the assembly property of the short peptide can represent that of the full-length Aβ.[50] Interestingly, this fragment involves two Phe residues, which would act as a hydrophobic core to initiate aggregation. If so, aggregation would be inhibited by the addition of trehalose because the side chains of these residues make complexes with the sugar, consequently avoiding direct contact between the Aβ chains. We are now investigating whether such a mechanism is valid or not, using MD simulations.

CONCLUSION

The physicochemical uniqueness of trehalose originates from the presence of an α,α-1,1-linkage, which brings about the rigid conformation with a clam, shell-like shape. Because of its conformational rigidity, trehalose has a unique hydration characteristic: a spatially anisotropic but dynamically stable hydration shell. As a result, dehydration pockets are formed on the top side of trehalose and it accepts hydrophobic molecules such as benzene without significant dehydration penalty, leading to the formation of a stable intermolecular complex as shown in Figures 5 and 8. Combining this study with our previous ones, it is evident that trehalose has an amphiphilic character, which brings about its multifunctional character as a stress protectant. This view would bring about a significant advance in exploiting further possibility of this sugar in scientific and industrial applications.

ASSOCIATED CONTENT

Supporting Information. (1) Probability vs reaction coordinate, (2) PMF curve obtained with a 2 ns umbrella simulation for each window, (3) comparison of the molecular motions about the glycosidic linkage between trehalose and neotrehalose, and (4) figures for structures A−D in Table 2. This material is available free of charge via the Internet at http://pubs.acs.org.

AUTHOR INFORMATION

Corresponding Author
*E-mail: msakurai@bio.titech.ac.jp.

Present Addresses
[§]Faculty of Health Science, Department of Health and Nutrition, Osaka Aoyama University, 2-11-1 Niina, Minoh City, Osaka 562-8580, Japan.

■ ACKNOWLEDGMENT

This work was supported in part by the Program for Promotion of Basic Research Activities for Innovative Biosciences (PROBRAIN) and also in part by Grants-in-Aid for Scientific Research on Priority Areas (No. 21370068) from the Ministry of Education, Culture, Sports, Science, and Technology of Japan.

■ REFERENCES

(1) Elbein, A. D. *Adv. Carbohydr. Chem. Biochem.* **1974**, *30*, 227–256.
(2) Laere, A. V. *FEMS Microbiol. Rev.* **1989**, *63*, 201–210.
(3) Singer, M. A.; Lindquist, S. *TIBTECH* **1998**, *16*, 460–468.
(4) Argüelles, J. C. *Arch. Microbiol.* **2000**, *174*, 217–224.
(5) Sakurai, M.; Furuki, T.; Akao, K.; Tanaka, D.; Nakahara, Y.; Kikawada, T.; Watanabe, M.; Okuda, T. *Proc. Natl. Acad. Sci. U.S.A.* **2008**, *105*, 5093–5098.
(6) Crowe, J. H.; Carpenter, J. F.; Crowe, L. M. *Annu. Rev. Physiol.* **1998**, *60*, 73–103.
(7) Crowe, J. H. In *Molecular Aspects of the Stress Response: Chaperones, Membranes and Networks*; Csermely, P., Vígh, L., Eds.; Landes Bioscience and Springer Science and Business Media: New York, 2007; Chapter 13.
(8) Oku, K.; Chaen, H.; Fukuda, S.; Kurimoto, M. *Nippon Shokuhin Kagaku Kougaku Kaishi* **1999**, *46*, 319−322.
(9) Benaroudj, N.; Lee, D. H.; Goldberg, L. A. *J. Biol. Chem.* **2001**, *276*, 24261–24267.
(10) Oku, K.; Kurose, M.; Kubota, M.; Fukuda, S.; Kurimoto, M.; Tujisaka, Y.; Sakurai, M. *Nippon Shokuhin Kagaku Kougaku Kaishi* **2003**, *50*, 133−137.
(11) Oku, K.; Watanabe, H.; Kubota, M.; Fukuda., S.; Kurimoto, M.; Tujisaka, Y.; Komori, M.; Inoue, Y.; Sakurai, M. *J. Am. Chem. Soc.* **2003**, *125*, 12739–12748.
(12) Oku, K.; Kurose, M.; Kubota, M.; Fukuda., S.; Kurimoto, M.; Tujisaka, Y.; Okabe, A.; Sakurai, M. *J. Phys. Chem. B* **2005**, *109*, 3032–3040.
(13) Herdeiro, R. S.; Pereira, M. D.; Panek, A. D.; Eleutherio, E. C. A. *Biochem. Biophys. Acta* **2006**, *1760*, 340–346.
(14) Tvaroška, I.; Vaclavik, L. *Carbohydr. Res.* **1987**, *160*, 137–149.
(15) Dowd, M. K.; Reilly, P. J.; French, A. D. *J. Comput. Chem.* **1992**, *13*, 102–114.
(16) Donnamaria, M. C.; Howard, E. I.; Grigera, J. R. *J. Chem. Soc., Faraday Trans.* **1994**, *90*, 2731–2735.
(17) Liu, Q.; Schmidt, R. K.; Teo, B.; Karplus, P. A.; Brady, J. W. *J. Am. Chem. Soc.* **1997**, *119*, 7851–7862.
(18) Sakurai, M.; Murata, M.; Inoue, Y.; Hino, A.; Kobayashi, S. *Bull. Chem. Soc. Jpn.* **1997**, *70*, 847–858.
(19) Bonanno, G.; Noto, R.; Fornili, S. L. *J. Chem. Soc., Faraday Trans.* **1998**, *94*, 2755–2762.
(20) Conrad, P. B.; Pablo, J. J. *J. Phys. Chem. A* **1999**, *103*, 4049–4055.
(21) Engelsen, S. B.; Pérez, S. *J. Phys. Chem. B* **2000**, *104*, 9301–9311.
(22) Kuttel, M. M.; Naidoo, K. J. *Carbohydr. Res.* **2005**, *340*, 875–879.
(23) Lerbret, A.; Bordat, P.; Affouard, F.; Descamps, M.; Migliardo, F. *J. Phys. Chem. B* **2005**, *109*, 11046–11057.
(24) Choi, Y.; Cho, K. W.; Jeong, K.; Jung, S. *Carbohydr. Res.* **2006**, *341*, 1020–1028.
(25) French, A. D.; Johnson, G. P.; Keltere, A.-M.; Dowd, M. K.; Cramer, C. J. *J. Phys. Chem. A* **2002**, *106*, 4988–4997.
(26) Brown, G. M.; Rohrer, D. C.; Berking, B.; Beevers, C. A.; Gould, R. O.; Simpson, R. *Acta Crystallogr.* **1972**, *B28*, 3145–3158.
(27) Jeffrey, G. A.; Nanni, R. *Carbohydr. Res.* **1985**, *137*, 21–30.
(28) Duda, C. A.; Stephens, E. S. *J. Am. Chem. Soc.* **1990**, *112*, 7406–7407.
(29) Duda, C. A.; Stephens, E. S. *J. Am. Chem. Soc.* **1993**, *115*, 8487–8488.
(30) Batta, G.; Kövér, K. E.; Gervay, J.; Horyák, M.; Roberts, G. M. *J. Am. Chem. Soc.* **1997**, *119*, 1336–1345.
(31) Rudolph, B. R.; Chandrasekhar, I.; Gaber, B. P.; Nagumo, M. *Chem. Phys. Lipids* **1990**, *53*, 243–261.
(32) Palma, R.; Himmel, M. E.; Brady, J. W. *J. Phys. Chem. B* **2000**, *104*, 7228–7234.
(33) Sakon, J.; Adney, W. S.; Himmel, M. E.; Thomas, S. R.; Karplus, P. A. *Biochemistry* **1996**, *35*, 10648–10660.
(34) Spezio, M.; Wilson, D. B.; Karplus, P. A. *Biochemistry* **1993**, *32*, 9906–9916.
(35) Sakon, J.; Irwin, D.; Wilson, D. B.; Karplus, P. A. *Nat. Struct. Biol.* **1997**, *4*, 810–818.
(36) Frisch, M. J.; Trucks, G. W.; Schlegel, H. B.; Scuseria, G. E.; Robb, M. A.; Cheeseman, J. R.; Montgomery, Jr., J. A.; Vreven, T.; Kudin, K. N.; Burant, J. C. et al. *Gaussian 03*, Revision E.01; Gaussian, Inc.: Wallingford, CT, 2004.
(37) Wang, J.; Wolf., R. M.; Caldwell, J. W.; Kollman, P. A.; Case, D. A. *J. Comput. Chem.* **2004**, *25*, 1157–1174.
(38) Jorgensen, W. L.; Chandrasekhar, J.; Madura, J. D.; Impey, R. W.; Klein, M. L. *J. Chem. Phys.* **1983**, *79*, 926–935.
(39) Kumar, S.; Bouzida, D.; Swendsen, R. H.; Kollman, P. A.; Rosenberg, M. *J. Comput. Chem.* **1992**, *13*, 1011–1021.
(40) Case, D. A.; Darde., T. A.; Cheatham, T. T.; Simmerling, C. L.; Wang, J.; Duke, R. E.; Luo, R.; Merz, K. M.; Wang, B.; Perlman, D. A. et al. *AMBER8*; University of California: San Francisco, 2004.
(41) Berendsen, H. J. C.; Postma, J. P. M.; van Gunstern, W. F.; Dinola, A.; Haak, J. R. *J. Chem. Phys.* **1984**, *81*, 3684–3690.
(42) Darden, T.; York, D.; Pedersen, L. *J. Chem. Phys.* **1993**, *98*, 10089–10092.
(43) Ryckaert, J. P.; Ciccotti., G.; Berendsen., H. J. C. *J. Comput. Phys.* **1977**, *23*, 327–341.
(44) Lucas, R.; Gómez-Pinto, I.; Aviñó, A.; Reina, J. J.; Eritja, R.; González, C.; Morales, J. C. *J. Am. Chem. Soc.* **2011**, *133*, 1909–1916.
(45) Tanaka, M.; Machida, Y.; Niu, S.; Ikeda, T.; Jana, N. R.; Doi, H.; Kurosawa, M.; Nekooki, M.; Nukina, N. *Nat. Med.* **2004**, *10*, 148–154.
(46) Arora, A.; Ha, C.; Park., C. B. *FEBS Lett.* **2004**, *564*, 121–125.
(47) Liu, R.; Barkhordarian, H.; Emadi, S.; Park, C. B.; Sierks, M. R. *Neurobiol. Dis.* **2005**, *20*, 74–81.
(48) Davies, J. E.; Sarkar, S.; Rubinsztein, D. C. *Hum. Mol. Genet.* **2006**, *15*, 23–31.
(49) Vilasi, S.; Iannuzzi, C.; Portaccio, M.; Irace, G.; Sirangelo, I. *Biochemistry* **2008**, *47*, 1789–1796.
(50) Morimoto, A.; Irie, K.; Murakami, K.; Masuda, Y.; Ohigashi, H.; Nagao, M.; Fukuda, H.; Shimizu, T.; Shirasawa, T. *J. Biol. Chem.* **2004**, *279*, 52781–52788.